

Effect Of Biosynthesized Iron Oxide Nanoparticles Against Anterior Flagella of *Leishmania Tropica*

Ahmed mahdi Barkash¹, Neama A. Ahmed², Fatin Muhammed Nawwab Aldeen³

^{1,2,3}Department of Biology, College of Science, University of Kirkuk, Iraq

Email: ahmedmahdy590@gmail.com

Abstract

Due to the importance of nanotechnology in medicine and its remarkable and significant development in the process of delivering treatment, in this study, iron oxide nanoparticles were bio-synthesized in the aqueous extract of the peels of the *Annona squamosa*, and then their inhibitory efficacy against the frontal flagella of the cutaneous *Leishmania tropica* parasite. Where the nanoparticles caused a decrease in parasite numbers within 96 hours of the start of growth, as well as a significant decrease in the total proteins of the parasite. (SEM), as well as infrared spectroscopy (FTIR), the results of XRD showed the size of the nanoscale (35) nanometers, as the biofabrication of nanoparticles is a safe and inexpensive method and one of the excellent factors for treatment.

1. Introduction

Leishmaniasis is a protozoal disease transmitted by vectors and caused by parasites of the genus *Leishmania*. It is a worldwide infectious disease that is increasing mortality and morbidity in various regions, primarily in the tropics and subtropics [1]. The World Health Organization (WHO) classified it as one of the most serious parasitic diseases, ranking second only to malaria. The parasitic protozoan life cycle is complex, with three major developmental stages: promastigotes, metacyclic-promastigotes, and amastigotes [2]. There are three main kinds of leishmaniasis: cutaneous leishmaniasis (CL), mucocutaneous leishmaniasis, and visceral or kala-azar leishmaniasis (VL) [3]. CL is distinguished by one or more ulcerating skin lesions. These heal slowly, have variable response rates to drug treatments, and can result in permanent and disfiguring scarring. CL is recognized as a severely stigmatizing skin disease as a result of this skin pathology [4]. The inclusion of inactive CL is significant because it is estimated that more than 40 million people are affected by the psychosocial effects of scarring caused by CL [5]. Because of their potent antimicrobial properties, nanoparticles have piqued the interest of scientists [6,7].

Nanobiotechnology is a new field of nanotechnology that uses nano-bio-based systems for biological applications such as therapeutic drug delivery, immunology, biotechnology, medicine, and engineering [8,9,10]. Nanoparticles are manufactured materials that contain particles in a free state or as an aggregate, and at least 50% of the particles have one or more dimensions in the range of 1-100 nm [11,12]. Nanoparticles are now the most important novel drug or gene vectors for cells, and they can help to advance drug delivery, medicine, and genetics [13,14,15]. One reason magnetic

nanoparticles are appealing is their potential application in medicine, health, and the environment, such as the enhancement of enzyme performance [16]. Chemical methods may endanger the environment and human health. Biosynthesis or green synthesis is an environmentally friendly and safe method for the synthesis of biological and natural compounds such as intracellular/extracellular extracts containing non-harmful microbial, plant, or fungi compounds [17].

2. Materials & Methods

2.1. Biosynthesis of Fe₂O₃ Nanoparticles

The plant extract of the peels of the fruit of the cream was prepared according to the method of Ul Ain et al. 10 g of the peels of the fruit were weighed and then boiled in 100 ml of distilled water at a temperature ranging from 50-70 °C with stirring. The sample was left at room temperature to cool down, and then the extract was first filtered using several layers of medical gauze, and then the extract was filtered for the second time using whatmans filter papers. by a Buechner funnel to get rid of the plant parts and fibers, and then it was centrifuged (Centrifuge) at (10000) rpm for 10 minutes) to get a pure supernatant free from impurities and small plant fibers. And then the plant extract is kept in clean and sterile glass bottles with a tight lid and at a temperature ranging from 4- to -10) until it is used in the study. I mixed the ternary iron ions (Fe + 3 and iron ions Fe + 2), as 1.35 g of FeCl₃.4H₂O of ferric chloride salt packed (0.7 g) of ferrous sulfate FeSO₄.7H₂O) was dissolved in 20 ml of well distilled Then (10 ml) of the plant extract was added in a ratio of 1: 2 to the vegetable solution and continued stirring, the extract was then stirred with different proportions of the hydrated iron salts of the fruit peels (1: 1), (2-1) and (1-2).) and (1-4) of the plant

extract and then heated by magnetic stirrer and adding a solution of NaOH (1.22) to the mixture in the form of slow distillation with continuous and rapid stirring for (50-30) minutes at a temperature of 70 degrees Celsius

Note the appearance of a black precipitate, where this precipitate appears at PH = 11 of iron oxide nanoparticles (Fe_2O_3) [18].part of the formed nanoparticles were dried in an electric oven at 80 ° C for about 4 hours, after which samples were sent for nanodiagnostic examinations.

2.2. Culture preparation according to Novy-Neal- Nicolle medium .

The promastigote forms of *Leishmania tropica* were cultured at 26 degrees Celsius in Novy-Neal-Nicolle (NNNN) medium, Anterior promastigote cutaneous leishmaniasis parasite was developed in a special biphasic culture medium called Tobie et al [19]at a temperature of 26° C. The medium is in the form of two phases, solid phase and liquid phase.

2.3. Methods and Instruments for Characterization

X-ray analysis (XRD) was performed to determine the size and type of nanoparticles, Fourier transform infrared spectroscopy (FTIR) spectroscopic analysis, as well as a transmission electron microscope examination to detect inside nanoparticles and scanning electron microscopy to detect the shape, surfaces and size of bio- The effect of nanoparticles manufactured by biological method was evaluated on the number of *Leishmania* parasite growth in the laboratory exposed to concentrations (10,20,30,40,) during (96) hours, after that the lowest and the highest inhibitory killer of *Leishmania tropica* were determined, as well as the inhibitory concentration of the text of the number was determined manufactured iron oxide nanoparticles inside the aqueous extract of fruit peels.

3. Result & Discussion

3.1. Characterization

XRD analysis of Fe_2O_3 iron oxide nanoparticles IONPs. In order to determine the nanoparticles and their crystal structure, where the results of X-ray diffraction showed in the form of regular clusters of high purity and few impurities, where a mixture of plant compounds and iron nanoparticles appeared, where peaks appeared as a result of the interaction that took place between nanoparticles of iron and aqueous extract to manufacture the particles Iron nanoparticles, and that the peaks that appeared at the corners, as we notice from Figure (1), actually gave five diagnosed peaks (31.503o, 35.341o, 56.321o, 45.306o, 75.15o), where they matched the X-ray diffraction measurements The peaks were of different intensity, ranging from medium to weak for iron nanoparticles, and these values correspond to the crystal levels (104, 116, 122, 214, 300) according to the database, according to the standard card

(JCPDS-79-1741) for X-ray diffraction. The expected crystalline shape of $\alpha\text{-Fe}_2\text{O}_3$ MNPs supermagnetic nanoparticles is consistent with the previous studies of Drbohlovova et al [20].

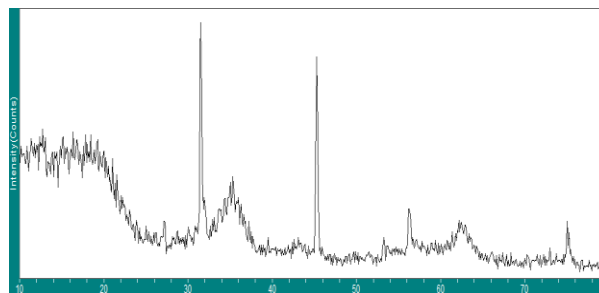


Figure (1) shows the X-ray diffraction of biosynthetic Fe_2O_3 SPIONs with the peels of the custard fruit.

Also, (FT-IR) Fourier Transform Infrared Spectroscopy analysis was conducted as shown in Figure (2 and 3) in order to identify the effective groups of the cream fruit peels and to predict their role in the synthesis of iron oxide nanoparticles and coating them with the plant extract helps in identifying the reducing molecules of iron oxide ions For both the nano iron oxide Fe_2O_3 and for the plant extract, where we notice from Figure (2) that the infrared spectrum of the aqueous extract of the fruit of the cream is from (4000 cm^{-1} to 450 cm^{-1}). And the appearance of bands at the top at (3437.29 cm^{-1} , 12098.95 cm^{-1} , 1637.06 cm^{-1}) 715.6 cm^{-1} , which refers to the (OH) hydroxyl group of water, also showed absorption bands at the tops (3630.59 cm^{-1} , 3435.66 cm^{-1} , 2079.57 cm^{-1} , 1654.52 cm^{-1} , 1637.72 cm^{-1} , 736.30 cm^{-1}), which refers to the hydroxyl group of the nanoparticles of oxide on which the extract of fruit peels is loaded, as in Figure (3), which refers to at 736.30 cm^{-1} - It is similar to the infrared spectrum of iron oxide nanoparticles made from the aqueous extract of the peels of the fruit of the cream as in Figure (2), which belongs to the Fe-O bond), and it is consistent with the previous study by Bukhari et al[21].

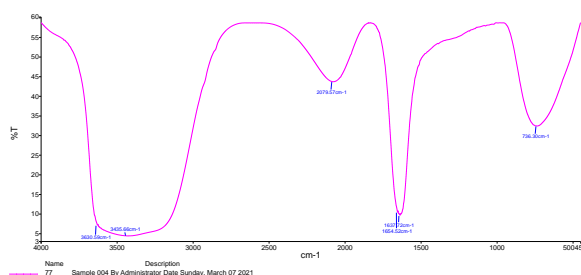


Figure (2) FT-IR spectra of the studied models of iron oxide nanoparticles

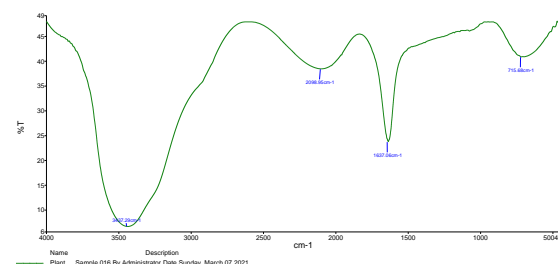
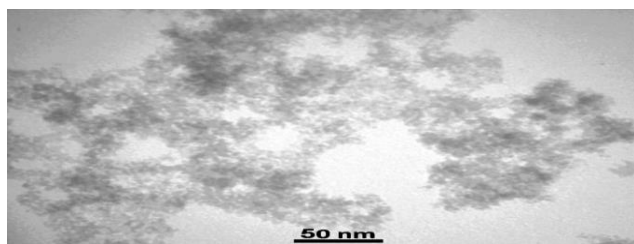


Figure (3) FT-IR spectra of the studied samples of the extract of the peels of an anemone fruit.

Transmission electron microscopy (TEM) analysis.

The size and shape of the nanoparticles are determined in order to obtain more information about the formed iron oxide nanoparticles, as it was analyzed through the TME examination of the examined particles. This examination is important to detect nanoparticles and determine the size and shape of the nanoparticles.

This assay shows nanoparticles that are prepared under (temperature 70-80) °C using TEM in order to obtain the actual size of (Fe2O3) MNPs with an average diameter of (50-10) nm as in the figure (4), which is an agreement Good with the result of XRD and also, where the results showed the presence of patterns of different shapes, but the spherical shape of the grains were dominant, and this is consistent with the examination of the scanning electron microscope (SEM) as in the figure (5), which showed the sizes of nanoparticles and nanoparticle thickness ranging between 20-33) nm and this agrees with both Khalil et al and Miri et al and Farahmandjou et al[22,23,24].



figure(4)TEM electron micrographs of Fe2O3 nanoparticles synthesized by biosynthesis

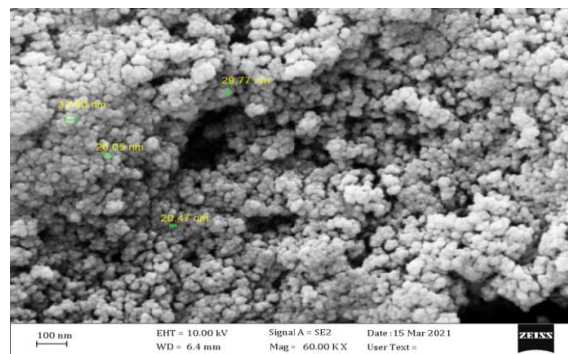


Figure (5) shows SEM images of Fe2O3 nanoparticles manufactured by biosynthesis.

3.2. Anti-Promastigote assay

As shown in the following tables 1, 2,3 and 4, the number of L. tropica promastigotes was gradually decreased by using a concentration of 10,20,30 and 40 mg/ml iron oxide nanoparticles bio-processed inside the aqueous extract of the custard fruit and when using different percentages of iron salts and The aqueous extract of fruit peel used in this research was used in different proportions, which are (1:1), (2:1), (1:2) and (1:4), and the inhibitory effect was observed after 96 hours of parasite growth with a percentage of (50,60,63,84),(43.5,50.2,69.1,74.3), (49.7, 51.7, 59.3, 69.3) and (52, 69.7, 79.2, 85.6) respectively. On the other hand, the total content of proteins was determined in L.tropica promastigotes, which was treated with IC50 for the manufactured nanoparticles.The results indicate that when the percentage of aqueous extract of fruit peels increases in the manufacture of nano iron oxide, the inhibition rate for the number of parasites increases.

Table No. (1) The effect of different concentrations of iron oxide nanoparticles manufactured by the biological method with a ratio of (1:1) on the numbers of frontal flagella of Leishmania parasite L.trobica

96			27			48			24			hourµg/ml
Inhibition %	%Growth	rate ±standard error	Inhibition %	%Growth	rate ±standard error	Inhibition %	%Growth	rate ±standard error	Inhibition %	%Growth	rate ±standard error	
0	100	84±0.028	0	100	76±0.0274	0	100	0.05± 64.5	0	100	± 0.05 59.5	control
50.8	49.2	39±0.0138	46.5	53.5	40±0.0087	0.3	99.7	0.017 ± 51.3	0.5	99.5	0.007 59.1±	10
60	40	33±0.0134	51.9	48.1	35±0.0074	30.9	69.1	± 0.019 40.1	2	98	50±0.0022	20
63.3	36.7	28±0.0189	67.3	32.7	35±0.0156	40	60	± 0.018 39.8	14.7	85.3	48±0.0059	30
84.2	15.8	22.3±0.19	78	22	26±0.0156	44.2	55.8	± 0.19 30.5	29.2	70.8	40±0.0072	40
60.2	39.8	33.9±0.02	59.1	40.9	38±0.0211	34.4	65.6	±0.028 45.2	13.1	86.9	52±0.0193	Pentostam

Table No. (2) shows the effect of different concentrations of iron oxide nanoparticles at a ratio of (2:1) of iron salts and aqueous extract of the peels of the bio-processed cream fruit on the number of L. tropica frontal flagella in different growth periods (hour)

96			72			48			24			Hour µg/ml
Inhibition %	Growth %	rate ±standard error	Inhibition %	Growth %	rate ±standard error	Inhibition %	Growth %	rate ±standard error	Inhibition %	Growth %	rate ±standard error	
0	100	84±0.028	0	100	76.4±0.027	0	100	0.05± 64.5	0	100	59.5 ± 0.05	control
43.5	56.5	0.016±30.0	39.7	57.3	0.016±32.8	28.5	71.5	0.026 ± 43.6	9.5	90.5	51.4± 0.004	10
50.2	49.8	0.016±28.9	50	50	±0.01831.5	47.5	52.5	± 0.018 40.4	15.8	84.2	46.1±0.014	20
69.1	30.9	0.014±27.4	64.8	35.2	±0.01529.8	49.5	50.5	0.014 ± 31.2	28.5	71.5	46.2±0.019	30
74.3	25.7	0.012± 22.6	74.1	25.9	±0.01528.2	64.5	35.5	± 0.019 30.2	36.7	63.3	40.2±0.012	40
64.2	35.8	33.9±0.012	50.1	49.9	38.1±0.021	27.4	72.6	±0.028 45.2	11.5	89.5	52.3±0.019	Pentostam

Table No. (3) Effect of different concentrations of iron oxide nanoparticles at a ratio (1: 2) on the number of *L. tropica* anterior flagella in different growth periods (hour)

96			72			48			24			hour(µg/ml)
Inhibition %	Growth %	rate ±standard error	Inhibition %	Growth %	rate ±standard error	Inhibition %	Growth %	rate ±standard error	Inhibition %	Growth %	rate ±standard error	
0	100	84±0.028	0	100	76.±0.0274	0	100	0.05 ±64.5	0	100	±0.0559.5	control
49.7	50.3	0.013±48.1	37.5	62.5	0.084±47.4	23	77	0.013±42.2	19.8	83.2	0.012 ±39.1	10
51.7	48.3	0.012±45.1	42.9	57.1	43.±0.0074	25.2	74.8	0.013±40.0	15	85	40.±0.0126	20
59.3	40.7	0.021±40.4	49.5	50.5	±0.01538.8	38.4	61.6	0.019 ±36.8	29.5	70.4	35.±0.0056	30
69.3	30.7	0.022 ±30.9	56.1	43.9	±0.01532.4	34.8	65.2	0.019 ±34.9	17	83	38.±0.0078	40
64.2	35.8	33.±0.0129	50.1	49.9	38.±0.0211	27.4	72.6	±0.02845.2	11.5	89.5	52.±0.0193	Pentostam

Table No. (4) shows the effect of different concentrations of iron oxide nanoparticles in a ratio of (4:1) biosynthesis on the number of *L. tropica* frontal flagella in different growth periods (hour)

96			72			48			24			hour(µg/ml)
Inhibition %	Growth %	rate ±standard error	Inhibition %	Growth %	rate ±standard error	Inhibition %	Growth %	rate ±standard error	Inhibition %	Growth %	rate ±standard error	
0	100	84±0.028	0	100	76.4±0.027	0	100	0.05± 64.5	0	100	59.5 ± 0.05	control
52	48.0	0.011±30.1	51.1	48.9	0.0833.2±	42.5	57.5	0.01939.±2	29.7	70.3	0.014 ±45.3	10
69.7	30.3	0.014±29.6	59.9	40.1	31.±0.0185	44.6	55.4	0.013 ±36.4	35.8	64.2	41.±0.0131	20
79.2	20.8	0.0217.6±	60.8	39.2	±0.01830.1	49.5	50.5	0.013 ±36.2	33.8	66.2	39.±0.0166	30
85.6	14.4	0.022 ±15.4±	79.2	20.8	±0.01623.2	56.9	43.1	0.016 ±29.6	38.7	61.3	33.±0.0125	40
64.2	35.8	33.±0.0129	50.1	49.9	38.±0.0211	27.4	72.6	±0.02845.2	11.5	89.5	52.±0.0193	Pentostam

The amount of protein was measured by following Lowry's method (Lowery et al[25], in the method of estimating the total protein of the Leishmania anterior flagella parasites that were treated by concentrations of magnetic iron oxide nano-extracts manufactured by the biological lethal method for half (IC50) the number of anterior flagella cells from the lineage Which were used in this study as shown in Table (5), as well as the protein measurement of

untreated cells by the concentrations used under study, where it was noted that the protein quantitative for the control, as well as for the ratios (1:1) and (1:2) and (2:1) and (4:1), respectively, ranged between (55.7, 39.6, 32.7, 28.3), where the amount of protein indicates a decrease after exposing the foregut parasites to the concentration of nanoparticles oxide, which has the role of killing half of the existing number (IC50).

Table (5) Effect of IC50 concentrations of iron oxide nanoparticle extract with different percentages of iron salts and aqueous extract of custard fruit on the amount of protein

µg/ml(IC50) µg/ml(Total.protein amountµg/ml	Inhibition percentage
control		60± 0.553	
(1:1) Rate	10	55.7± 0.495	30
(1:2) Rate	20	39± 0.411	39.9
(2:1) Rate	20	3650.32.7±	43.7
(4:1) Rate	10	2270.28.3 ±	47.7

It was noted in this study that the iron oxide nanoparticles used in this study affected the protein and metabolic efficiency of the cell. The treatment of Leishmania parasite *L. tropica* anterior flagella at IC50 concentration) of the nanoextract in the following ratios (1:1) and (2 -1) and (1-2) and (1-4), where a decrease in the amount of protein for the four different ratios and by (60, 55.7, 39.6, 32.7, 28.3) The results also indicated that the magnetic IONPs had inhibitory activity against the front phase of Leishmania parasite based on the concentrations, where it was observed that the rate of inhibition increased when using the ratio (4:1) of nanoparticles manufactured inside the plant extract, where the increase in the rate of cell death was from (52-86.6) during 96 hours, where the highest

percentage of parasite death was compared with the percentages used from the extract for nanoparticles, although the exact mechanism of iron oxide nanoparticles was not fully understood, it was suggested to clarify the future for their promising activities to combat Leishmania parasite, where the cell wall can be broken by Contacting or adhesion of nanoparticles to the cell wall of the parasite by oxidative potential with reactive oxygen and then releasing ions from the surfaces of nanoparticles Chen & Bothu and Lopez-Carballo [26,27]

Referemces

Abdukholikovich, S. A., Turakulovich, T. A., Abdullaevich, A. F., & Najmitdinovich, K. K. (2022).

Modern Views on Leishmaniasis Diagnosis, Preventive Measures and Treatment. *Central Asian Journal of Medical and Natural Science*, 3(5), 104-111.

Ullah, N., Nadhman, A., Siddiq, S., Mehwish, S., Islam, A., Jafri, L., & Hamayun, M. (2016). Plants as Antileishmanial Agents: Current Scenario. *Phytotherapy Research*.

World Health Organization P. WHO fact sheet on leishmaniasis: WHO; [updated 2020 March 2; cited 2020 April 04].

Kassi M, Kassi M, Afghan AK, Rehman R, Kasi PM. Marring leishmaniasis: the stigmatization and the impact of cutaneous leishmaniasis in Pakistan and Afghanistan. *PLoS Neglect Trop D*. 2008;2(10): e259.

ailley F, Mondragon-Shem K, Haines LR, Olabi A, Alorfi A, Ruiz-Postigo JA, Alvar J, Hotez P, Adams ER, Vélez ID, Al-Salem W. Cutaneous leishmaniasis and co-morbid major depressive disorder: a systematic review with burden estimates. *PLoS Neglect Trop D*. 2019;13(2): e0007092.

Mahmoud, W.; Elazzazy, A.M.; Danial, E.N. In Vitro Evaluation of Antioxidant, Biochemical and Antimicrobial Properties of Biosynthesized Silver Nanoparticles against Multidrug-Resistant Bacterial Pathogens. *Biotechnol. Biotechnol. Equip.* **2017**, *31*, 373–379. [[Google Scholar](#)] [[CrossRef](#)]

Hameed, A.S.H.; Karthikeyan, C.; Ahamed, A.P.; Thajuddin, N.; Alharbi, N.S.; Alharbi, S.A.; Ravi, G. In Vitro Antibacterial Activity of ZnO and Nd Doped ZnO Nanoparticles against ESBL Producing *Escherichia coli* and *Klebsiella pneumoniae*. *Sci. Rep.* **2016**, *6*, 24312. [[Google Scholar](#)] [[CrossRef](#)] [[PubMed](#)]

Khatami, M.; Mortazavi, S.M.; Kishani-Farahani, Z.; Amini, A.; Amini, E.; Heli, H. Biosynthesis of Silver Nanoparticles Using Pine Pollen and Evaluation of the Antifungal Efficiency. *Iran. J. Biotechnol.* **2017**, *15*, 95–101. [[Google Scholar](#)] [[CrossRef](#)]

Khatami, M.; Heli, H.; Jahani, P.M.; Azizi, H.; Nobre, M.A.L. Copper/Copper Oxide Nanoparticles Synthesis Using *Stachys lavandulifolia* and Its Antibacterial Activity. *IET Nanobiotechnol.* **2017**, *11*, 709–713. [[Google Scholar](#)] [[CrossRef](#)]

Poor, M.H.S.; Khatami, M.; Azizi, H.; Abazari, Y. Cytotoxic Activity of Biosynthesized Ag Nanoparticles by *Plantago Major* Towards a Human Breast Cancer Cell Line. *Rend. Lincei* **2017**, *28*, 693–699. [[Google Scholar](#)] [[CrossRef](#)]

Khatami, M.; Mehnipor, R.; Poor, M.H.S.; Jouzani, G.S. Facile Biosynthesis of Silver Nanoparticles Using *Descurainia Sophia* and Evaluation of Their Antibacterial and Antifungal Properties. *J. Clust. Sci.* **2016**, *27*, 1601–1612. [[Google Scholar](#)] [[CrossRef](#)]

Pulit-Prociak, J.; Banach, M. Silver Nanoparticles—A Material of the Future...? *Open Chem.* **2016**, *14*, 76–91. [[Google Scholar](#)] [[CrossRef](#)]

Singh, P.; Singh, H.; Castro-Aceituno, V.; Ahn, S.; Kim, Y.J.; Farh, M.E.-A.; Yang, D.C. Engineering of Mesoporous Silica Nanoparticles for Release of Ginsenoside Ck and Rh2 to Enhance Their Anticancer and Anti-Inflammatory Efficacy: In Vitro Studies. *J. Nanopart. Res.* **2017**, *19*, 257. [[Google](#)

[Scholar](#)] [[CrossRef](#)]

Selot, R.; Marepally, S.; Vemula, P.K.; Jayandharan, G.R. Nanoparticle Coated Viral Vectors for Gene Therapy. *Curr. Biotechnol.* **2016**, *5*, 44–53. [[Google Scholar](#)] [[CrossRef](#)]

Junejo, Y.; Güner, A.; Baykal, A. Synthesis and Characterization of Amoxicillin Derived Silver Nanoparticles: Its Catalytic Effect on Degradation of Some Pharmaceutical Antibiotics. *Appl. Surf. Sci.* **2014**, *317*, 914–922. [[Google Scholar](#)] [[CrossRef](#)]

Lunge, S.; Singh, S.; Sinha, A. Magnetic Iron Oxide (Fe₃O₄) Nanoparticles from Tea Waste for Arsenic Removal. *J. Magn. Magn. Mater.* **2014**, *356*, 21–31. [[Google Scholar](#)] [[CrossRef](#)]

El-Kassas, H.Y.; Aly-Eldeen, M.A.; Gharib, S.M. Green Synthesis of Iron Oxide (Fe₃O₄) Nanoparticles Using Two Selected Brown Seaweeds: Characterization and Application for Lead Bioremediation. *Acta Oceanol. Sin.* **2016**, *35*, 89–98. [[Google Scholar](#)] [[CrossRef](#)]

Ul Ain, Q., Islam, A., Nadhman, A., & Yasinzai, M. (2020). Comparative analysis of chemically and biologically synthesized iron oxide nanoparticles against *Leishmania tropica*. *bioRxiv*, 829408.

Chang k and Bray R (1985). *Biology of Leishmaniasis*. In: *Leishmaniasis*. Chang k and Bray R. Elsevier science pub. Amsterdam. New Yourk, Oxford. Pp: 1-130.

Drbohlavova, J., Hrdy, R., Adam, V., Kizek, R., Schneeweiss, O., & Hubalek, J. (2009). Preparation and properties of various magnetic nanoparticles. *Sensors*, 9(4), 2352-2362.

Bukhari, A., Ijaz, I., Gilani, E., Nazir, A., Zain, H., Saeed, R., ... & Naseer, Y. (2021). Green synthesis of metal and metal oxide nanoparticles using different plants' parts for antimicrobial activity and anticancer activity: a review article. *Coatings*, 11(11), 1374.

Khalil, A. T., Ovais, M., Ullah, I., Ali, M., Shinwari, Z. K., & Maaza, M. (2017). Biosynthesis of iron oxide (Fe₂O₃) nanoparticles via aqueous extracts of *Sageretia thea* (Osbeck.) and their pharmacognostic properties. *Green Chemistry Letters and Reviews*, 10(4), 186-201.

Miri, A., Najafzadeh, H., Darroudi, M., Miri, M. J., Kouhbanani, M. A. J., & Sarani, M. (2021). Iron oxide nanoparticles: biosynthesis, magnetic behavior, cytotoxic effect. *ChemistryOpen*, 10(3), 327-333.

Farahmandjou, M., & Soflaee, F. (2015). Synthesis and characterization of α-Fe₂O₃ nanoparticles by simple co-precipitation method. *Physical Chemistry Research*, 3(3), 191-196.

Lowry, O. H., Rosebrough, N. J., Farr, A. L., & Randall, R. J. (1951). Protein measurement with the folin phenol reagent *J BiolChem* 193: 265–275.

Chen, K. L., & Bothun, G. D. (2014). Nanoparticles meet cell membranes: probing nonspecific interactions using model membranes.

Lopez-Carballo, G., Higuera, L., Gavara, R., & Hernández-Muñoz, P. (2013). Silver ions release from antibacterial chitosan films containing in situ generated silver nanoparticles. *Journal of agricultural and food chemistry*, 61(1), 260-267.